An In-Depth Assessment of Internal Contamination in the Wide Field/Planetary Camera

Republished from the Journal of the IES *May-June 1990 issue, pages 29-35*

Carl Maag, Jerry Millard, and Mark Anderson
Jet Propulsion Laboratory, California Institute of Technology

Abstract

Following thermal vacuum/thermal balance testing, a gray haze was discovered on the corners of the Wide Field/Planetary Camera (WF/PC) aperture window. The phenomenon was suggested to be a result of molecular transport from a low outgassing structural adhesive. Detailed analyses, both chemical and analytical, were conducted to assess the formation of the haze. Each material was considered individually, as it was not known if the actual contamination was a result of one, many, or possibly none of the materials considered. Results of the analytical assessment and the comparison with the aforementioned chemical analyses provided incontrovertible evidence as to the cause of the window haze. The resultant cleanup and subsequent elimination of the problem are also addressed. [Editor's Note: This 1990 paper is republished as part of the *Journal of the IEST* 50th anniversary celebration. It is accompanied by remarks from Patti Hansen, author of "Overview of the HST Contamination Engineering Program at 15 Years: A Cleanliness Metric for Success with Optical Satellites" paper in this issue.]

KEYWORDS

Hubble Space Telescope, Wide Field/Planetary Camera, outgassing, contamination, modeling, chemical analysis

COMMENTS BY PATTI HANSEN

Patti Hansen, author of "Overview of the HST Contamination Engineering Program at 15 Years: A Cleanliness Metric for Success with Optical Satellite" in this issue and a senior staff engineer at the Jet Propulsion Laboratory, successfully developed and directed the implementation of the contamination control programs for the HST program. Hansen was asked to review this 1990 paper. Here are her comments:

This is a great paper; the topic is relevant today. This was one of the first papers published to detail the analysis used to identify the source of an observed contamination on a flight optic.

Contamination engineers, more than 20 years later, continue to use these types of analyses to determine contaminant species and, as in this case, use the results of the analyses to determine the source(s) of the contaminants. Similar analyses were used in the post-mission analysis of the WFPC1 pick-off mirror as reported in my paper. These analyses are detailed in "Contamination-induced Degradation of Optics Exposed to the Hubble Space Telescope Interior," Tveekrem et al.; "Contamination Effects of EUV Optics," Tveekrem; and "Effects of the Space Environment on the HST Wide Field Planetary Camera-I," MacKenty et al. [references 17, 18, and 19 in the current Hansen paper].

As for the relevance to HST, I have found it ironic that the post-mission analyses of this instrument's pick-off mirror used similar analyses to determine the cause of the observed contamination.

It is my understanding that this paper was recognized by IEST for computer modeling. [The paper received a Maurice Simpson Technical Editors Award in 1991.] To quote my paper, "The HST Contamination Control Program utilized detailed contamination modeling and trade studies to compare risk of potentially contaminating the HST and its scientific instruments during servicing mission activities. The results were used to craft the flight rules for each servicing mission." The contamination analyses have become "standard" for contamination-sensitive missions to provide data to perform trade studies and define acceptable outgassing rates to meet on-orbit performance.

An In-Depth Assessment of

Internal Contamination in the Wide Field/Planetary Camera

By: Carl Maag*, Jerry Millard, and Mark Anderson
Jet Propulsion Laboratory
California Institute of Technology
Pasadena, California

ABSTRACT

Following thermal vacuum/thermal balance testing, a gray haze was discovered on the corners of the Wide Field/Planetary Camera (WF/PC) aperture window. The phenomenon was suggested to be a result of molecular transport from a low outgassing structural adhesive. Detailed analyses, both chemical and analytical, were conducted to assess the formation of the haze. Each material was considered individually, as it was not known if the actual contamination was a result of one, many, or possibly none of the materials considered. Results of the analytical assessment and the comparison with the aforementioned chemical analyses provided incontrovertible evidence as to the cause of the window haze. The resultant cleanup and subsequent elimination of the problem are also addressed.

INTRODUCTION

The Wide Field/Planetary Camera (WF/PC) is one of five science instruments integrated into the Hubble Space Telescope (HST). The WF/PC uses eight charge-coupled devices (CCDs) as imaging sensors in the wavelength region from 1,200 to 10,000 Angstrom. The WF/PC is encased in a structure that shields the optics from the external environment and provides mounting for both the internal electronics and the radiator. Figure 1 shows a cutaway diagram of the camera. As can be seen, the incoming energy is reflected from a mirror (pick-off mirror) through an entrance aperture at the front end of the camera and ultimately into the cameras through a series of refractive and reflective optical elements.

The WF/PC has been subjected to six system-level thermal vacuum tests at the Jet Propulsion Laboratory (JPL) and one at the Lockheed Missile and Space Company, Inc. (LMSC) while installed in the HST. Following the test at LMSC, a gray haze was discovered on two corners of the WF/PC aperture window. Figure 2 shows the extent of the deposition. At the time of notation, it was not possible to determine if the haze was on the inside or outside of the aperture window. A decision was made to remove the window, take wipe samples of the surrounding areas, and transport the window to JPL for further analyses.

CONTAMINATION ANALYSIS (SPECTRAL/CHEMICAL)

Upon receipt of the window at JPL, detailed spectral and chemical analyses were conducted to determine the source of the haze. The detailed visual inspection of the window, performed after removal from the WF/PC, indicated that the haze was restricted to the inside of the window. The wipe samples taken from both sides of the window confirmed that the outside was relatively clean (<1 mg/ft^2) compared with the inside (>10 mg/ft^2). The spectral transmission measurements (throughput) of the hazed areas showed a loss of transmission at the shorter wavelengths (<3000Å). The clear areas of the window showed no significant transmission loss.

The chemical analysis of the aperture window can be divided into the following categories:

1. Atomic absorption spectroscopy (AA) to determine the presence of magnesium.
2. Ion chromatography (IC) to determine the presence of anions such as fluoride, chloride, nitrates, and sulfates.
3. Gel-permeation chromatography/high performance liquid chromatography (GPC/HPLC) to determine the molecular weight of the contamination.
4. Fourier transform infrared (FTIR) spectroscopy.
   a. transmission through the window.
   b. diffuse reflectance for trace organic analysis of the solvent removed material.

The aperture window, made of magnesium fluoride, was first examined without altering the surface by transmission infrared spectroscopy through the window. This revealed that the affected areas had aliphatic (CH containing) organic functional groups present which

Keywords: Hubble Space Telescope, Wide Field/Planetary Camera, outgassing, contamination, modelling, chemical anaylsis

*Carl Maag is currently employed at Science Applications International Corporation, Glendora, California

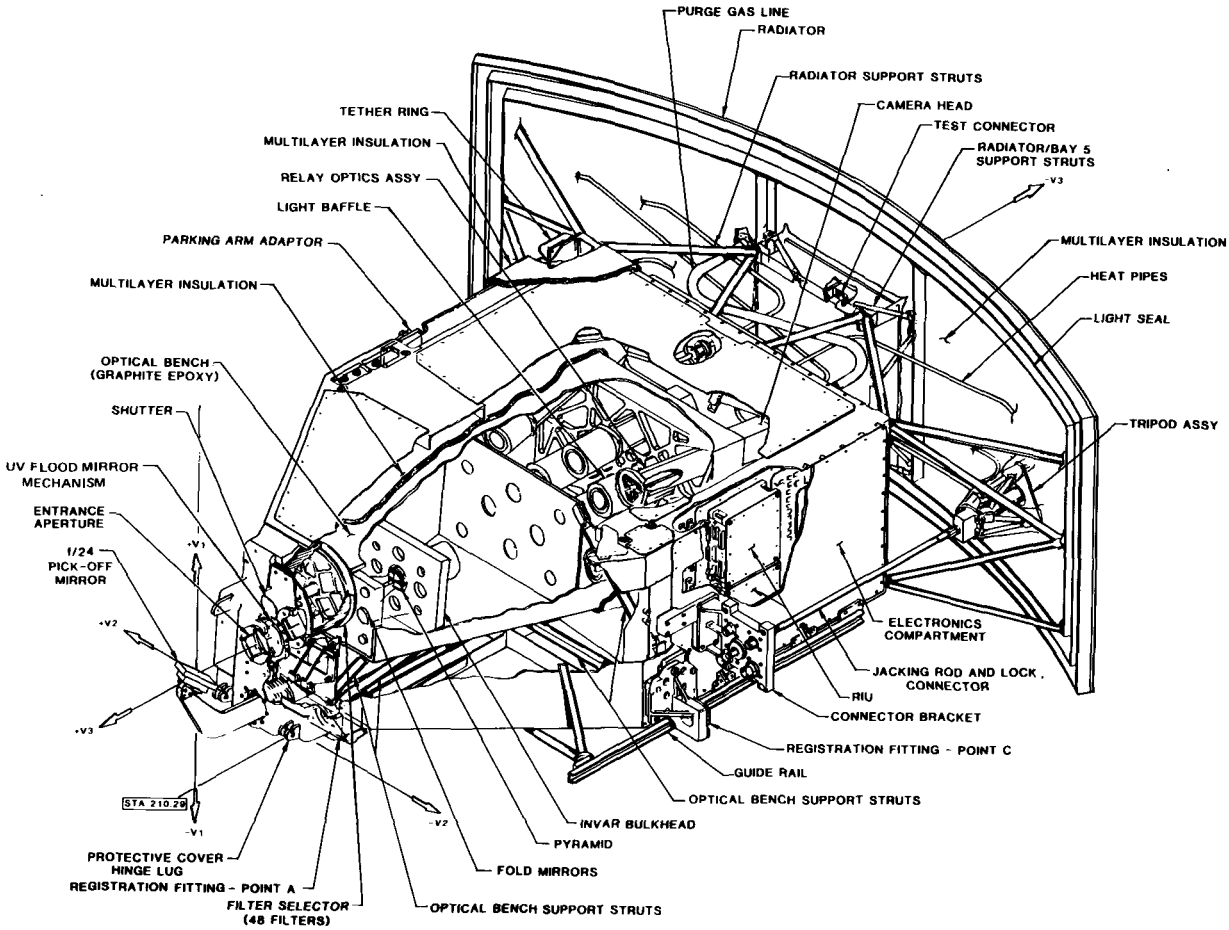

Figure 1. Cutaway diagram of the camera.

absorb at approximately 2900 cm^{-1}. The unaffected areas had no significant absorption at this wavelength. The magnesium fluoride window absorbs strongly in the mid-infrared region which limited organic functional group analysis using this method.

In order to further analyze the contamination, the haze was removed by sequentially rinsing the window with methylene chloride and ethanol. The haze was visually removed following the ethanol rinse, indicating it was a polar material. The solutions were analyzed by both AA for magnesium and IC for fluoride and other anions. No significant amount of these species was found, indicating that the contamination did not react chemically with the window.

The rinse solution was then analyzed by gel permeation chromatography. This technique separates unknowns into peaks, depending on molecular size. From this, the molecular weight can be estimated. The chromatographic analysis showed that the haze was a complex mixture with a broad molecular weight distribution (see Figure 3).

The contamination was next analyzed by diffuse reflectance FTIR and compared with suspected sources. In this method, the sample is evaporated from a solvent onto an infrared transparent, finely divided, potassium chloride powder. This provides a matrix that allows multiple reflections of infrared radiation through the sample and increases the sensitivity of the FTIR spectrometer. This method provided an excellent infrared spectrum of the aperture window contamination (see Figure 4).

Concurrent with these analyses, a review of the hardware interior exposed to the aperture window was conducted. The window is mounted in a structure called the WF/PC flight mechanical cover assembly, hereafter referred to as the mechanical cover. Attached to the mechanical cover is an assembly called the quantum efficiency hysteresis (QEH) mirror mechanism, also called the UV flip-mirror mechanism.

The QEH mirror mechanism shown in Figure 5 required a modification late in the hardware flow that precluded an additional bakeout of the structure. This modification consisted of the addition of the optics installation and a fracture control modification. The optics installation operation used a very small quantity of room temperature vulcanizing silicone (RTV) to

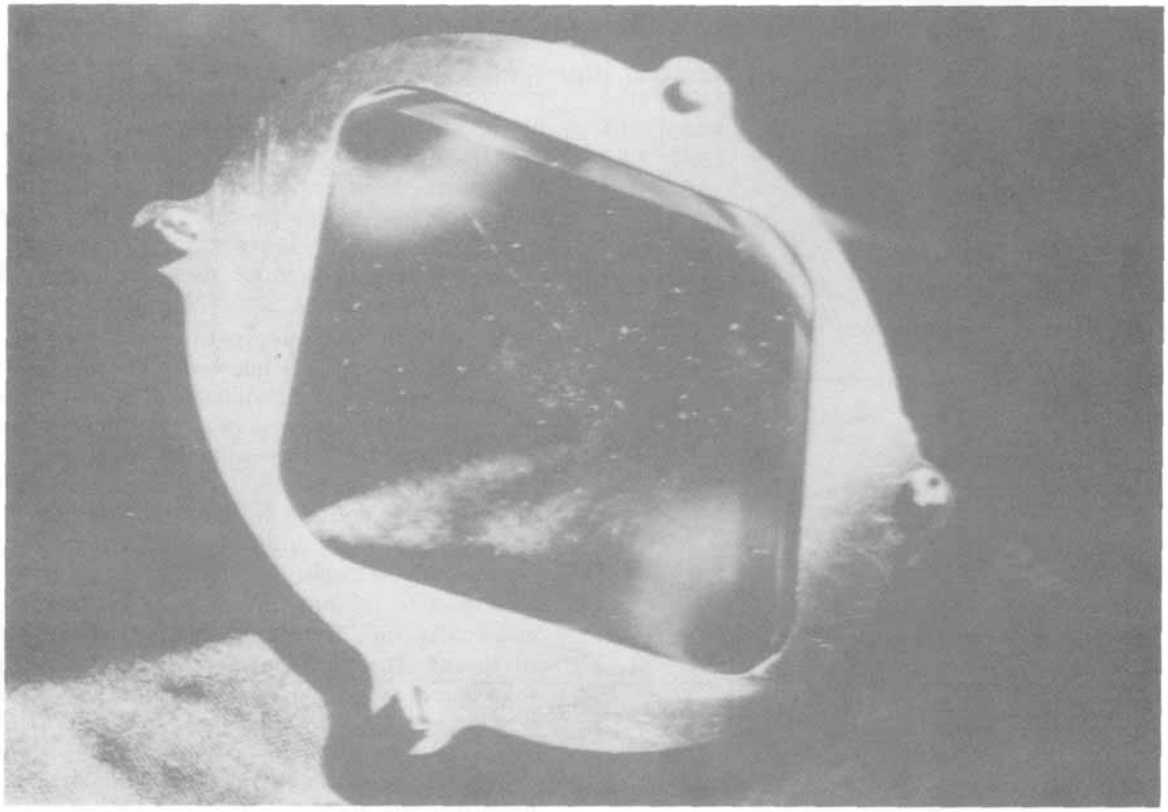

Figure 2. Window in retaining cap showing molecular contamination pattern.

mount the mirror assembly. The fracture control operation used a Stycast 2850 and a Dacron lacing cord, MIL-T-43435. The lacing cord was used as lanyards in three locations on the QEH mirror mechanism. Approximately 4 in. of the lacing cord and several "dots" of Stycast were used to bond the cord. All materials used in this modification were selected with the utmost care from the NASA approved materials list to preclude contamination. The QEH mirror mechanism had been baked several times at both the subsystem and component levels. The mechanism was in an extremely clean condition prior to the optics installation operation and fracture control modifications as evidenced by the absence of organic precipitates on the liquid nitrogen cold plate typically installed during bakeout procedures.

CONTAMINATION ANALYSIS (ANALYTICAL)

An analytical study was conducted to evaluate the molecular contamination distribution deposited on the inside surface of the aperture window in the forward housing (housing for flip-mirror assembly for QEH system and shutter mechanism). Its purpose was to determine if candidate materials (i.e., Stycast 2850 adhesive and Dacron lanyard material used on the flip-mirror hinge assembly) outgassing could have caused the deposition pattern observed on the window and, if not, from where did the outgassing have to originate within the housing to cause the observed pattern. The origin of the outgasing was determined by comparing the deposition pattern on the window (evidenced by photographs) with the computed analytical distributions for candidate sources.

The leading candidate materials were the Stycast adhesive and the lanyard material used at the hinge points of the flip-mirror assembly (see Figure 5). The flip-mirror is to the left, and the controlling mechanism to the right. The hinges are in the foreground. On the lower hinge, the white lanyard material is held in place by wire and dark Stycast adhesive. Although not visible, the same is true for the top hinge.

This entire assembly resides within the forward housing, and the hinges are very close to the inside of the aperture window, each having a good view of the window. Figure 5 shows the flip-mirror in the QEH operating position. During camera operation, the flip-mirror is positioned farther to the left, allowing light to travel through the window and between the flip-mirror and the controlling mechanism. The camera shutter is behind this assembly.

The analysis approach was to perform a simplified computer simulation of the outgassing of each of the materials and to record individually the mass distribution created on the window as a result. These results were compared with the actual deposition patterns on the window, as revealed by photographs.

Pk. No.	Ret. Time	Area	Area %	Peak Mol. Wt.	Mw	Mn	Mw/Mn	Mz
2	11.68	754952	18.0500	787	896	877	1.0225	916
3	16.00	1218965	29.1439	259	320	311	1.0296	331
4	16.40	818021	19.5579	234	219	218	1.0033	219
5	18.23	789953	18.8868	146	141	140	1.0084	142
6	20.00	177961	4.2548	93	92	92	1.0017	92
7	20.91	258584	6.1824	73	70	70	1.0049	70
8	22.55	164132	3.9242	48	45	45	1.0061	46
Total Area: 4182570			Area Reject: 56919		One sample per 1.002 sec.			

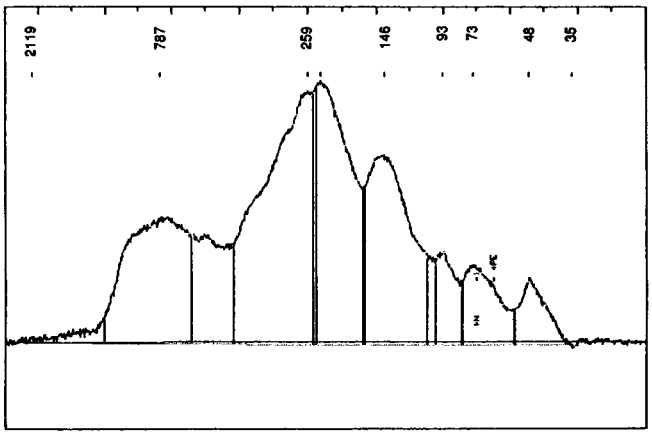

Figure 3. Molecular weight chromatogram.

This approach required the construction of a detailed geometric mass transport model of the interior of the housing, and the careful evaluation of the window deposition photographs.

Several photographs were taken of the window deposition with variations in angle and lighting. This caused a significant variation in the observed deposition pattern. A large number of photographs were studied in order to understand the true scope and distribution of the deposition.

Figure 2 is the best single photograph of the contamination pattern on the inside of the window. A careful study of several photographs revealed the true extent of the contamination. The entire exposed surface of the window was contaminated. Two corners of the window received the most extensive deposition (a corner is defined as the region in the vicinity of the window retaining cap curvature). A window-wide pattern to the contamination exists. The most extensively contaminated corners are those closest to the hinges. Here, the contamination approaches a maximum. The least contamination occurs in the corners farthest from the hinges.

It should be noted that in the immediate corners there is less contamination than in the region around the corners (the image of a "baseball field" pattern is seen in the most contaminated corners in Figure 2.) A wide, sloping ridge of relatively moderate contamination tends to extend out from the most extensively contaminated corners, being minimized near the center of the window, but slightly to one side of the centerline of the window (where the centerline extends between the most extensively contaminated corners). Several photographs are required to see this total pattern.

Although similar, the two most extensively contaminated corners do not have identical patterns (i.e., one corner may be contaminated more than another). This overall deposition pattern suggests the contamination source is relatively close to the window within the housing enclosure.

A quantitative deposition distribution of the contamination on the window was not achievable because of previous window handling and cleaning. As a result, the pattern revealed by photographs formed a qualitative map to match for analytical comparison purposes.

A lumped-parameter multinodal mass transport model of the housing interior was created in order to compute the distribution of outgassed mass to interior surfaces of the enclosure. The JPL CAP computer code was used to perform the outgassing simulation.[1] This code performs free molecular flow mass transport involving surface source emission and deposition reemission as well as engine plume impingement and venting.

In order to compute a deposition distribution with adequate resolution, a detailed geometric model was required. The resulting model consisted of 245 nodes, including candidate outgassing materials. It was also required to understand where additional cleaning might be needed to remove contamination from other areas of the enclosure. The following high-resolution nodal breakdown was used:

- 63 nodes for the flip-mirror/mechanism assembly and hinges.
- 27 nodes for the internal housing structure and aft aperture entrance.
- 48 nodes for the internal retaining cap for the window.
- 64 nodes for the internal window surface.
- 25 nodes to represent regions of Stycast adhesive around hinges.
- 18 nodes to represent regions of lanyard around hinges.

The Stycast and lanyard materials are located in various places around both hinge assemblies. The determination of the precise positions and geometries for these materials was scaled from design drawings and numerous photographs of the materials in place.

Figure 6 shows a plot of the window and retaining cap nodal resolution with the window recessed slightly within the cap. Figure 7 shows a plot of the entire nodal model which illustrates the proximity of the geometry involved, especially the hinges with respect to the window.

A precise quantitative deposition pattern on the window could not be computed because the required kinetic mass properties of the materials were not known

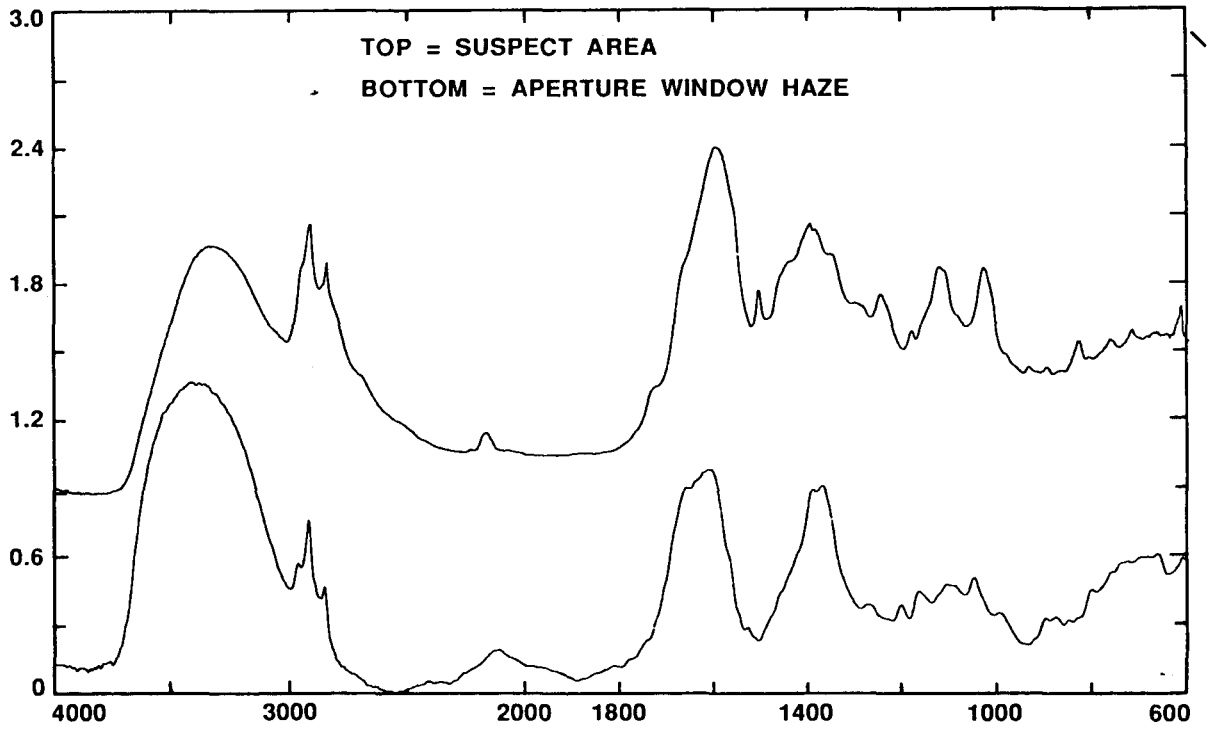

Figure 4. FTIR spectra.

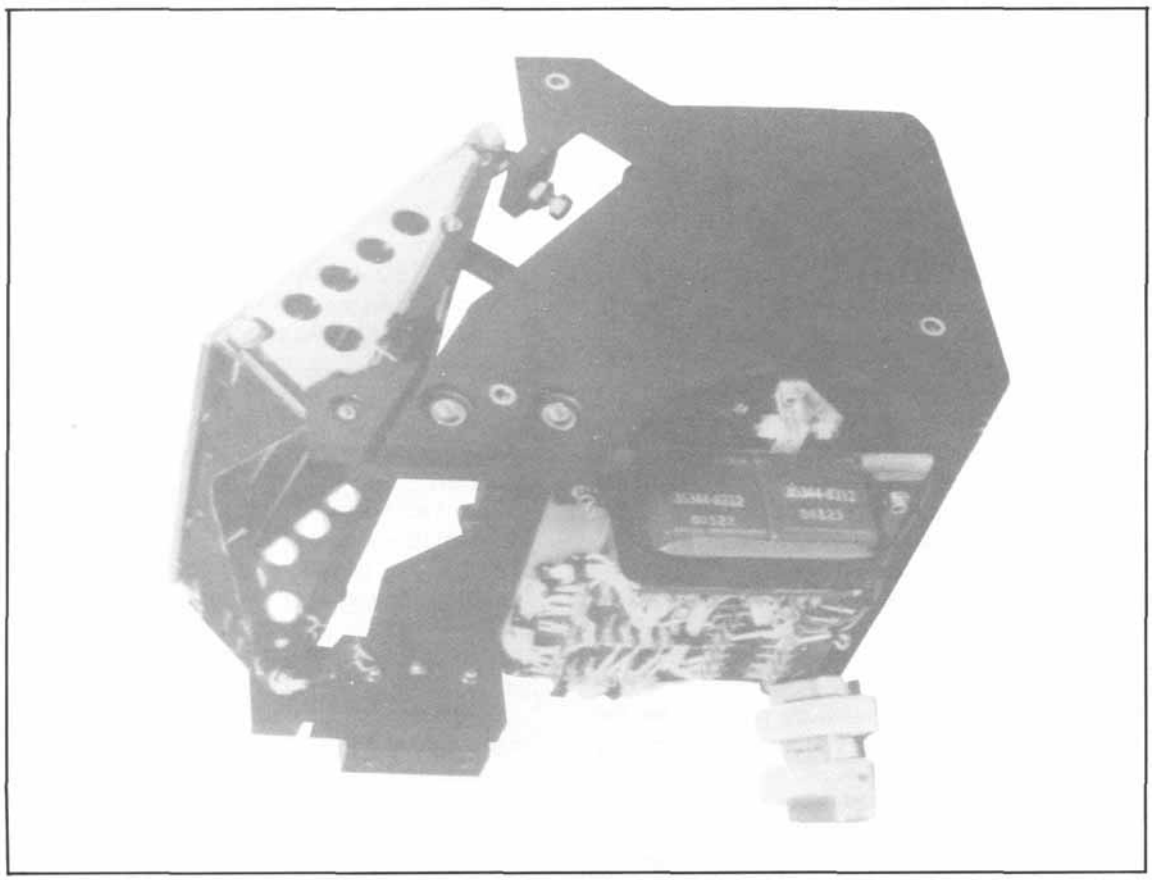

Figure 5. Flip-mirror assembly with hinges in foreground.

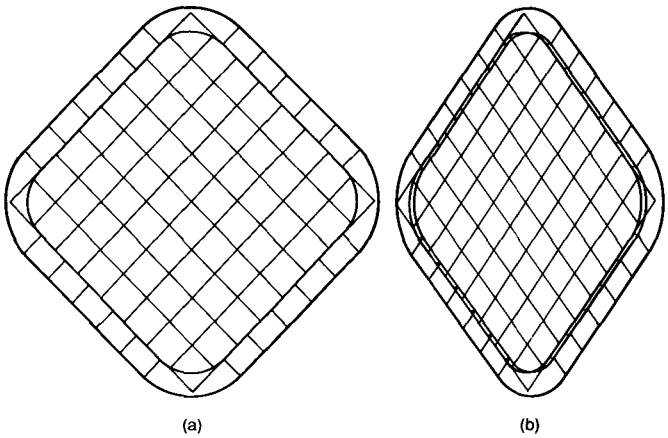

Figure 6. Internal view of window and retaining cap nodal model: (a) front view, (b) off-axis view.

(typically these must be derived from specific experimental test data) and the detailed temperature history of the housing could not be reconstructed. As a result, several analysis assumptions were made consistent with the limitations of the problem:

- Only the Stycast and lanyard materials were allowed to outgas.
- The mass emission distribution of each material followed a cosine distribution.
- All incident mass on a surface was assumed to stick permanently.
- Each material was assumed to be of uniform composition.
- Each material was evaluated individually.

As a result of these assumptions, the resulting solutions were the distribution of the emitted masses by direct line-of-sight throughout the housing. The results for each material were normalized assuming a value of 1.0 for the minimum deposition value on a window node. As a result, deposition distributions for each material are relative to this value. These results do not provide a direct comparison of the relative amount of deposition from each material. In other words, these results do not directly show if one material is far more contaminating than another. Laboratory tests and the comparisons of the computed deposition patterns on the window to the actual patterns are required for that determination.

It must be remembered that it was possible that neither of the prime candidate materials was responsible for the window contamination. The analysis resolved that issue.

The resulting normalized deposition patterns on the window are shown in Figure 8. These results are presented individually for the Stycast adhesive (a) and the lanyard material (b). In both cases, the entire window experiences deposition.

The results for the lanyard material are symmetrical about the horizontal centerline of the window. They also show the pattern of being the highest near the top and bottom corners, decreasing slightly in these corners. The side corner regions display the lowest values. In addition, there is a ridge formation in the vertical pattern which peaks far to the mechanism side of the window. These results show a deposition variation over the surface of the window of approximately a factor of 13.7.

The results for the Stycast adhesive are similar, except the ridge tends to be less skewed to the mechanism side and has a trend up the middle of the window. In addition, the distribution is not symmetrical about the horizontal centerline. Instead, it tends to be moderately biased toward the lower half of the window. These results show a deposition variation over the window surface of approximately a factor of 7.5.

A careful qualitative comparison of the results for each material with the actual pattern from the photographs suggests the Stycast adhesive is the dominant source of deposition. The analytic results for this material match the pattern significantly better than the lanyard results.

An investigation of other geometric regions of the housing enclosure that might outgas and produce a similar deposition pattern on the window resulted in the conclusion that this is extremely unlikely. Model results show the pattern is virtually impossible to reproduce from other geometric regions of the housing. Also, there is a limited number of places in the housing having material with the potential to create such a problem. In addition, given realistic kinetics, an unlikely temperature profile history for the window would have to be assumed.

A side benefit of this analysis was that it provided information as to where in the housing enclosure surface samples (wipes) should be taken for laboratory analysis of deposited contamination.

SUMMARY AND CONCLUSIONS

The outgassing model showed that relatively small areas (where Stycast epoxy bonding material was used) were suspected as sources of contamination. These areas, as well as those predicted to have deposits similar to the window, were solvent extracted. Diffuse reflectance FTIR was then used for comparison with the haze material.

The two infrared spectra (See Figure 4) show the same major organic functional groups present, and samples to be of similar mixtures. The organic functional groups of amine, aliphatic, and hydroxyl predominate the spectra. This is consistent with the fact that the Stycast bonding material is an aliphatic amine cured epoxy.

The analytical chemistry data support the conclusion that vacuum outgassing of the Stycast bonded area was responsible for the aperture window haze.

Although the individual evaluations could not conclusively establish the source of the deposition, they provided incontrovertible evidence as to the source when combined.

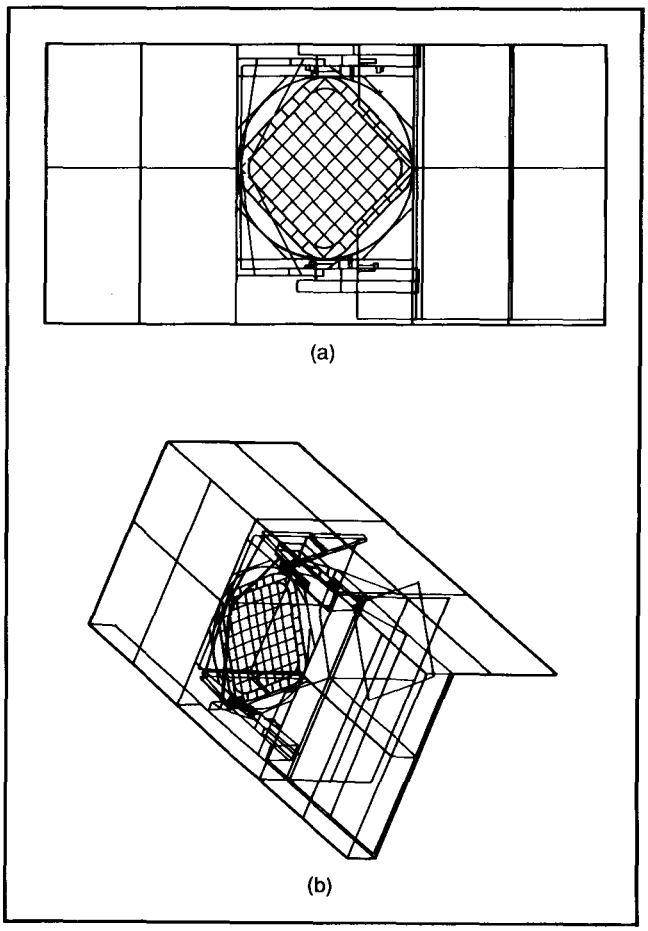

Figure 7. Plots of the entire nodal model: (a) front view, (b) off-axis view.

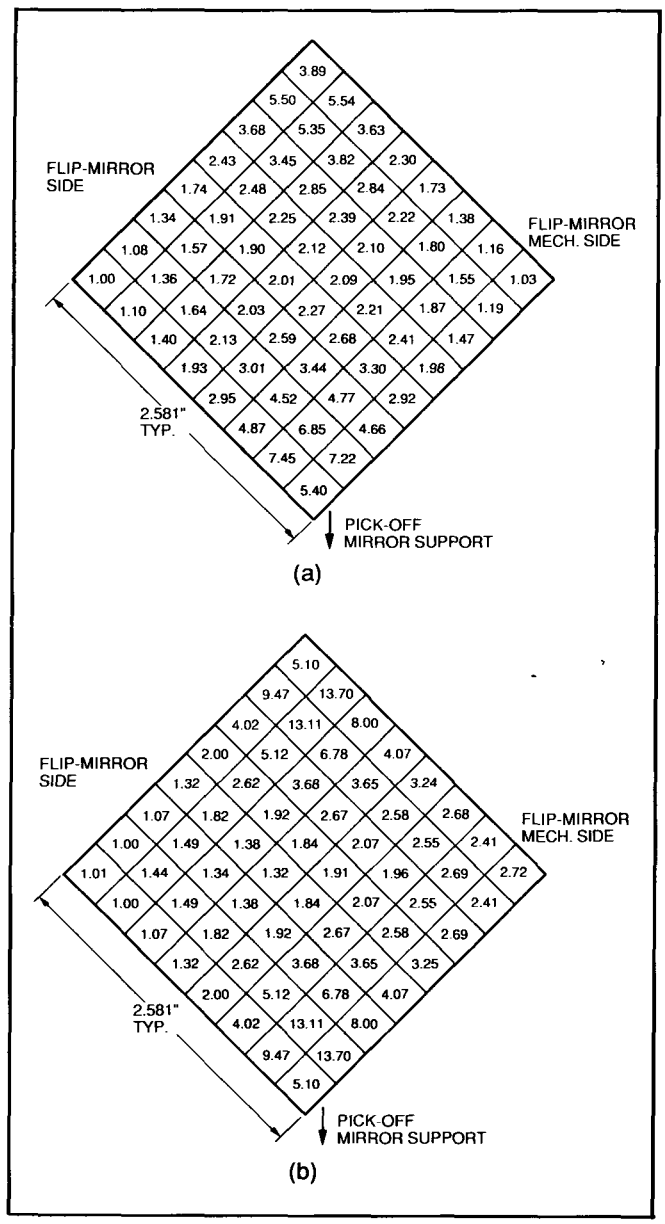

Figure 8. Analytical deposition pattern on window from: (a) Stycast adhesive outgassing, (b) Lanyard outgassing.

The mechanical cover was later subjected to a 45°C (113°F) bakeout using two temperature-controlled quartz crystal microbalances (TQCMs) to monitor any additional outgassing. The bakeout continued for 45 days at which time the data from the TQCMs suggested all outgassing had decreased to an acceptable level (i.e., less than the established requirement).

Both analytical and chemical analysis can provide useful data in the resolution of critical contamination issues. When used together, the techniques provide the analyst or systems engineer with solid unquestionable data. In addition, this entire incident reinforces the fact that handbooks, such as those containing outgassing information, should be used only as guidelines, particularly when dealing with near or far UV optics.

This work has been carried out by the Applied Technologies Section, Jet Propulsion Laboratory, California Institute of Technology, and was sponsored by the National Aeronautics and Space Administration.

REFERENCE

1. Millard, J.M., *Jet Propulsion Laboratory Contamination Analysis Program–Programmer and User Manual*, JPL Report No. 715-55, prepared by the Jet Propulsion Laboratory for the Goddard Space Flight Center, August (1980).